Electron-hole dynamics in normal and deuterated KH_2PO_4 illuminated by intense femtosecond laser pulses

Guillaume Duchateau,[1,*] Ghita Geoffroy,[2] Anthony Dyan,[1] Hervé Piombini,[1] and Stéphane Guizard[3]

[1]*Commissariat à l'Energie Atomique, Centre d'Etudes du Ripault, BP 16, F-37260 Monts, France*

[2]*CELIA and Commissariat à l'Energie Atomique/IRAMIS/SPAM, Université Bordeaux 1, 351 Cours de la Libération, F-33405 Talence, France*

[3]*Commissariat à l'Energie Atomique/IRAMIS/Laboratoire des Solides Irradiés, F-91191 Gif-sur-Yvette, France*

(Received 16 July 2010; revised manuscript received 13 November 2010; published 22 February 2011)

The dynamics of electrons and holes in potassium dihydrogen phosphate (KH_2PO_4 or KDP) crystals and its deuterated analog (KD_2PO_4 or DKDP) induced by femtosecond laser pulses is investigated at $\lambda = 800$ nm. To do so, experiments based on a femtosecond time-resolved interferometry technique have been carried out. It is shown that two relaxation dynamics exist in KDP and DKDP crystals. Both of them correspond to physical mechanisms for which the multiphoton order required to promote valence electrons to the conduction band is lower than the one of a defect-free crystal. These results suggest the presence of states located in the band gap that may be due to the presence of defects existing before any laser illumination or created in the course of interaction. In order to interpret the experiments, a model based on a kinetic equation system has been developed. Modeling results are in good agreement with the experimental data.

DOI: 10.1103/PhysRevB.83.075114 PACS number(s): 72.20.Jv, 79.20.Ws, 71.55.−i

I. INTRODUCTION

Potassium dihydrogen phosphate (KH_2PO_4 or KDP) and its deuterated analog (KD_2PO_4 or DKDP) are dielectric materials commonly used to convert laser light to shorter wavelengths. However, laser-induced damage in these materials remains a limiting factor in the development of high-power laser systems designed to produce inertial confinement fusion.[1] Indeed, these crystals are used to produce the 3ω pulses ($\lambda = 351$ nm) required to induce an efficient energy deposition into a target made of a deuterium-tritium mixture. These pulses have an average fluence close to 10 J/cm^2 and a duration of roughly 3 ns, which results in pulses exhibiting low intensities of a few GW/cm^2. Despite such features, it has been shown that laser-induced damage (LID) appears in the bulk of (D)KDP crystals, which is detrimental for the laser aperture.[1] Therefore, in order to improve the laser flux resistance of these crystals, there is a need to understand the underlying physical mechanisms responsible for LID.

LID is localized, i.e., the crystal is not damaged uniformly. It is thus assumed that the LID originates from precursor defects (enhancing the laser absorption) that may be present within the crystal before any laser illumination or that appear during the course of interaction. Some of these defects have been identified, but their relation to LID in the nanosecond time scale has not been clearly established yet. The defects created are essentially connected with the proton transport within the hydrogen bond network. This displacement induces various types of point defects, e.g., deuterium or hydrogen interstitial atoms D^0/H^0, oxygen vacancies for which a hole is trapped next to them, and $[HPO4]^-$ centers ($[DPO4]^-$ in DKDP) for which a hole is trapped next to the hydrogen-deuterium vacancy. The latter species are often called A radicals. Well-known defects in KDP crystals are also the B radicals that consist of a self-trapped hole (STH) associated with the $[H2PO4]^0$ center ($[D2PO4]^0$ in DKDP). See, for instance, Refs. 2–6 and references therein for a more detailed description of these defects. Above the picosecond time scale, the defect recombination appears to be governed by a thermally-activated diffusive process.[7]

The LID of (D)KDP crystals have been studied both experimentally and theoretically in the nanosecond time scale (see, for example, Refs. 8–14). The evolution of the fluence required to reach a given damage level with respect to the laser wavelength shows a striking feature: this fluence evolves by successive plateaus,[8] which can be explained by introducing states located in the band gap (SLG).[15,16] Nevertheless, because of the nanosecond time scale, the previous studies only provide poor information about the precursor defects. Indeed, the long time that elapses after the initial absorption, during which an efficient nucleus activity has occurred, gives rise to a loss of information about the precursor defects. In this framework, femtosecond time-resolved experiments are clearly of great interest, and ultrashort pulses present at least two advantages. First, they allow us to expose the sample to much higher intensities. For wide-band-gap dielectrics, this means it is possible to excite efficiently a large density of carriers by a nonlinear process, subsequently increasing the sensitivity of any probing experiment. Second, by performing a time-resolved experiment, it is possible to decompose and to get a much clearer view of the successive mechanisms. To our knowledge, two experiments have been carried out in this femtosecond domain for KDP crystals: Davis *et al.*[17] used a pump-probe technique, providing indications of the system dynamics, and Carr *et al.*[18] performed spectroscopic measurements during the optical breakdown.

In order to further understand the physical mechanisms leading to LID in (D)KDP crystals and to improve the knowledge about the fundamental electronic mechanisms involved in these dielectric materials, we have carried out studies in the femtosecond time scale, allowing us to follow the initial steps of electronic relaxation and atomic rearrangements. The experiment, described in Sec. II, consists of a femtosecond time-resolved interferometry technique that was

successfully used to investigate the relaxation dynamics in various materials.[19,20] We have chosen to deal with $\lambda = 800$ nm in order to be able to vary the laser intensity in a large range before reaching the ablation threshold. Also, this allows us to accurately determine the order of the multiphoton process, which can shed light on the presence of SLG. Further, this experiment allows measuring the relaxation dynamics of the photoexcited bulk electrons in both KDP and DKDP crystals. It is shown that the relaxation dynamics can depend on the laser intensity and the isotope under consideration. We concentrate on the importance of self-trapping of electrons and holes in the defect creation process. These experimental results are reported in Sec. III, where a first analysis of the data makes it possible to introduce a modeling approach aimed at describing the previously mentioned mechanisms. In order to finely analyze these results, we have developed in Sec. IV a model based on a kinetic equation system (KES) that predicts the time evolution of the electronic densities associated with the various states. The comparison between experimental and modeling results renders it possible to evaluate the generalized multiphoton absorption cross sections and the capture cross section, which are shown to depend on the electron kinetic energy. Conclusions are drawn in Sec. V, and a few analyses are reported in the Appendixes for the reader's convenience.

II. EXPERIMENTAL PROCEDURES

Experiments were performed with KDP and DKDP single crystals manufactured by Saint-Gobain. The DKDP crystal was grown by slowly cooling a supersaturated solution of KDP and heavy water. The KDP crystal was prepared under fast-growth conditions. Both of them have high optical quality. The crystal was oriented far away from the phase matching angle and was moved after each measurement point; that is, each data point was measured on a fresh site. We used the Saclay Laser-matter Interaction Center-LUCA laser facility of the CEA Saclay.[21] This laser delivers pulses of duration $\tau_L = 55$ fs (full-width half-maximum, FWHM) of 30 mJ at 800 nm (1.55 eV), but less than 1 mJ is needed for our experiment. The laser temporally gated to have a single-shot beam that is divided into two fractions; one part is the pump pulse, and the second fraction, the probe pulse, is divided in two parts in a Michelson-type interferometer before being focused onto the sample.

The principle of this experiment is described in detail in Ref. 20 and is based on interference fringes in the frequency domain obtained when two collinear femtosecond pulses separated by a fixed time delay (whose maximum value is $\Delta t = 90$ ps in this experiment) are observed at the exit of a monochromator. The fringe system is recorded by a charge-coupled device camera, and a Fourier analysis allows us to extract the phase and amplitude information for the probe beam that has crossed the sample. When a high-intensity pump pulse is focused on the sample at some time between the two probe pulses, the fringes are distorted due to the material index modifications, and their contrast decreases. As a consequence, the induced phase shift $\Delta\Phi$ between the two probe pulses can be measured as a function of time by changing the delay between the pump pulse and the probe pulses. Within the Drude model, $\Delta\Phi$ is expressed as[20]

$$\Delta\Phi = \frac{2\pi L}{\lambda}\left\{n_2 I + \frac{e^2}{2n_0\varepsilon_0}\left[-\frac{f_{cb}n_{cb}}{m^*\omega^2} + \frac{f_{tr}n_{tr}}{m\left(\omega_{tr}^2 - \omega^2\right)}\right]\right\}, \quad (1)$$

where L is the effective length over which the index is modified, λ is the wavelength of the probe beam, I is the intensity of the pump laser, n_2 is the nonlinear index, n_{cb} is the density of conduction electrons, f_{cb} is the oscillator strength for the transitions occurring in the conduction band (CB), n_{tr} is the density of electrons trapped in the band gap, $\hbar\omega_{tr}$ corresponds to the energy difference between the fundamental and the first excited state of the induced defect and f_{tr} is its corresponding oscillator strength, ω is the laser frequency of the probe beam, m is the electron mass, and m^* is the electron effective mass in the conduction band.

The measurement of $\Delta\Phi$ with respect to the time delay between the pump and the probe pulse gives access to the evolution of quantities n_{cb} and n_{tr} with respect to time and, thus, information on the physical mechanisms of excitation, defects creation, and relaxation. The first term of Eq. (1) represents the Kerr effect, which induces a real positive contribution since $\Delta n_{Kerr} = n_2 I$ and n_2 is positive. It gives both the zero time delay and the experimental time resolution, which is of the order of 120 fs (FWHM). The second term, which is proportional to the density of electrons that have been excited by the pump pulse in the conduction band, is always negative. The last term stands for the trapping of the electrons subsequent to a defect formation. It can be positive or negative, depending on the sign of $(\omega^2 - \omega_{tr}^2)$. The time-dependent n_{cb} can be separated from the Kerr effect since in most cases the lifetime of the free carriers is longer than the laser-pulse duration. Hence, just after the pump pulse, the maximum value of the negative phase shift corresponds to the total number of carriers excited by the pump pulse.

III. EXPERIMENTAL RESULTS

For both crystals and for a wide range of pump intensities we have measured the phase shift $\Delta\Phi$ at various time delays between the pump and probe laser beams. The chosen wavelength is 800 nm in order to be able to vary the laser intensity over a large range before reaching the ablation threshold, which is measured to be about 68 TW/cm^2 (waist of 64 μm). In this way, an accurate determination of the order of the multiphoton process is possible, which gives interesting information on the presence of SLG.

For KDP, we present in Fig. 1 the phase shift and the absorption with respect to the time delay up to 1500 fs after the multiphoton excitation induced by the laser pump with $I = 60$ TW/cm^2. Just after zero delays, the fast generation of free carriers is demonstrated by both the negative value of the phase shift and the strong absorption in the crystal. It appears that the dynamics of the electronic relaxation follows two kinetics, and $\Delta\Phi$ can be fitted at first glance by two exponential time decays where the fast relaxation time τ_1 is around 300 fs and does not depend on the intensities considered in this paper. This behavior is characteristic of the fast trapping of an exciton (self-trapped exciton, STE),[19,20] as observed in various insulators. Experimental evidence of the formation of STE in KDP has been given by Ogorodnikov,[5] who has attributed a

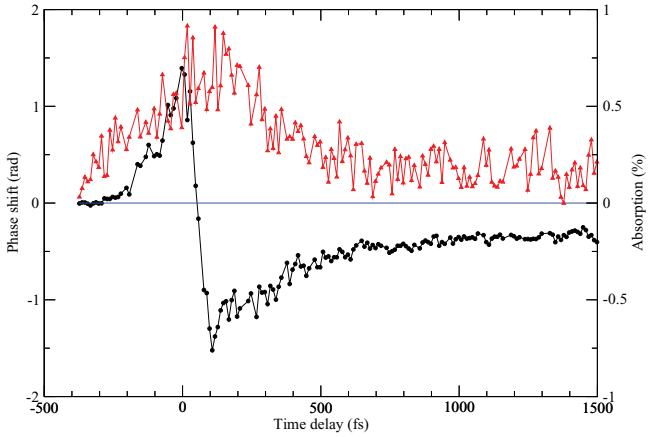

FIG. 1. (Color online) Evolution of the phase shift (top black curve) and the absorption (bottom red curve) as a function of the time delay for a KDP crystal and a laser intensity of roughly 60 TW/cm^2.

luminescence at 5.24 eV to the radiative recombination of the STE, following excitation by VUV photon from synchrotron radiation. It should also be noted here that the fast relaxation time τ_1 in KDP is comparable to the one measured in SiO_2, KBr, and NaCl. Figure 2 shows the same results as in Fig. 1 but with longer time delays. In order to evaluate the relaxation times, we use a fitting function based on exponentials, such as $\alpha e^{-\Delta t/\tau_1} + \beta e^{-\Delta t/\tau_2}$, where α, β, τ_1, and τ_2 are fitting parameters. From this kind of measurement, it appears that the second relaxation time τ_2 varies roughly as I^{-1}, where I is the laser intensity, and has a range of tens of picoseconds. For instance, for $I = 60$ TW/cm^2, we found $\tau_2 \simeq 8$ ps for KDP, with a root-mean-square relative error (RMSRE) close to 5%. This fit has been performed in the range $\Delta t \in [0;20$ ps] in order to avoid the Kerr effect and the trapping that cannot be described by the above fitting function based on decreasing exponentials. Further, note that the obtained value of τ_2 slightly depends on the delay time range used. Furthermore, as usual, it is worth noting that the fitting procedure only provides trends since there is no reason for the time delay to evolve with the used fitting function. Actually, as will be shown in Sec. IV, the evolution of the phase shift with respect to the time delay is much more complex than a simple superposition of exponential behaviors. Figure 2 also shows that the phase shift becomes positive after roughly 40 ps. This latter value corresponds to defect formation times for which free electrons are trapped in the $\hbar\omega_{\rm tr}$ level. Indeed, this corresponds to the positive contribution of the last term of Eq. (1).

In order to study the isotopic effect, the evolution of the phase shift with respect to the time delay for KDP and DKDP is given by Fig. 3. Because of the experimental setup, it was not possible to obtain data with exactly the same laser intensity for both crystals. Also, we used $I = 42.32$ TW/cm^2 and $I = 36.8$ TW/cm^2 for KDP and DKDP, respectively; these values are sufficiently close to allow a comparison to make sense. The phase shift for DKDP has the same shape as that of KDP; that is, it exhibits a fast and a slow relaxation dynamics. An analogous study made in DKDP reveals the same behavior as in KDP with the same value for τ_1 ($\simeq$300 fs), suggesting that this value does not depend on the nature of the isotope present in the material. The phase shift reaches the zero value for a time

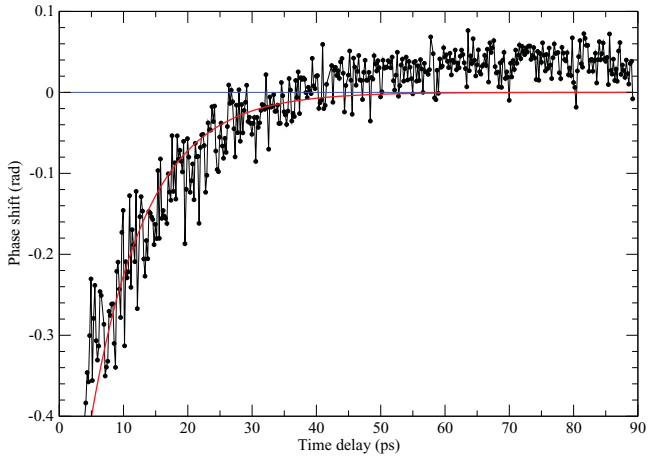

FIG. 2. (Color online) Same as Fig. 1 but with longer time delays. The smooth red curve is a fit to evaluate the relaxation time (see text for more details).

delay close to 50 ps, indicating a slower relaxation kinetics than for KDP. More precisely, a fit based on the previously described function indicates that τ_2 is close to 10 and 18 ps for KDP and DKDP, respectively, with RMSRE close to 15%. The resulting fitting curves are shown in Fig. 3. Also, it appears that τ_2 is almost twice as long for DKDP than for KDP. This factor can only be reasonably assigned to an isotopic influence since when dealing with intrinsic mechanisms, the only difference between KDP and DKDP is that protons are replaced by deuterons. Furthermore, this type of influence associated with the isotope effect has already been observed in the literature; see, for instance, Refs. 5,7,17, and 22. Also, it is worth noting that we are presently dealing with a migration process following a hydrogen bond breaking and not dealing with a decoherence occurring after a few vibrational periods. As long as the migration process takes place, the dielectric function evolves. Unlike a relaxation process due to a decoherence occurring after a few vibrational periods for which the isotopic influence is to introduce a factor $\sqrt{2}$[23], there is no clear

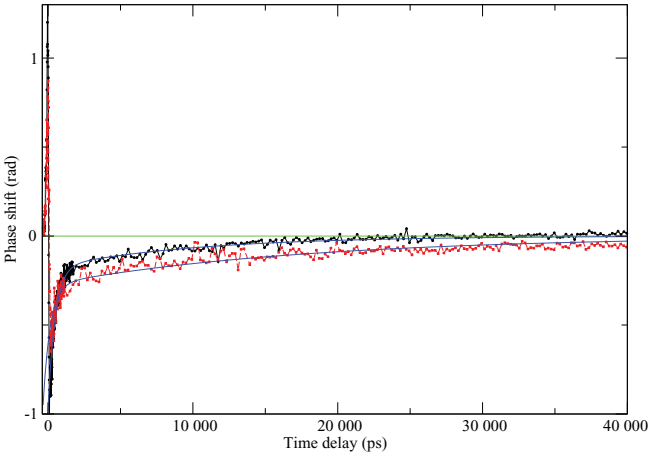

FIG. 3. (Color online) Evolution of the phase shift as a function of the time delay for KDP (solid black curve) and DKDP (dashed red curve) crystals. The laser intensities are $I = 42.32$ TW/cm^2 and $I = 36.8$ TW/cm^2 for KDP and DKDP, respectively. The smooth blue curves are fits of the data (see text).

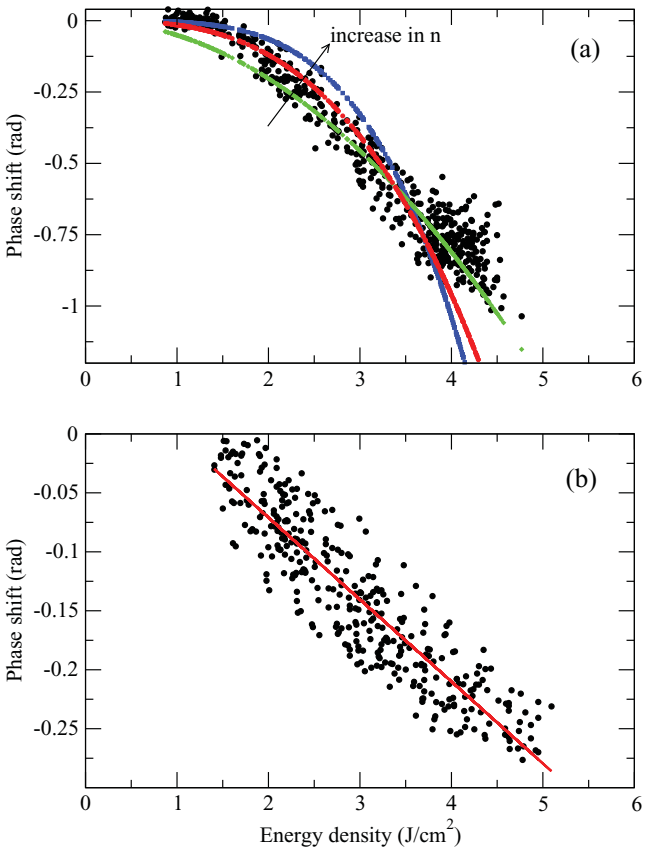

FIG. 4. (Color) Evolution of the phase shift as a function of the laser energy density at (a) $\Delta t = 150$ fs and (b) $\Delta t = 20$ ps in a DKDP crystal. The red (medium gray) curves are the best fits of the experimental data with a power law. For $\Delta t = 150$ fs, the green (light gray) and blue (dark gray) curves are fits with a power law with an exponent equal to 2 and 4, respectively. Note that for the highest energy densities, a deviation from the power-law behavior is observed because the damage threshold is reached. It turns out that the corresponding plasma density strongly absorbs and reflects the probe beam, and the measurement does not make sense in these conditions.

interpretation of the observed factor 1.8. Nevertheless, we propose that during its migration, the proton or deuteron has to get over potential barriers, possibly by tunneling.[17,22] Since the probability of getting over a potential barrier is larger when the particle mass is small, the proton migrates more easily than the deuteron, resulting in a faster relaxation dynamics for KDP. Despite using a different experimental setup, Davis *et al.* have also measured a factor close to 2 between relaxation signals of KDP and DKDP.[17]

To investigate the presence of intermediate states that may play a role in the excitation mechanism, we have determined the order of the multiphoton process. To identify this order, we measured the phase shift as a function of the intensity of the pump pulse at a fixed delay time. These results are reported in Fig. 4 for a DKDP crystal. (The results are similar for a KDP crystal and therefore are not presented here.) The data reported in Figs. 4(a) and 4(b) correspond to time delays of 150 fs and 20 ps, respectively, i.e., the fast and the slow dynamics, respectively. For both KDP and DKDP, we found that the phase shift evolves as I^n with $n = 3$ for $\Delta t = 150$ fs. Note that the experimental data do not only account for the excitation process at high intensities due to the formation of a dense plasma absorbing and reflecting the laser pulses. Also, the fits have been performed for energy densities lower than 3.9 J/cm^2 (the value for which no significant experimental artifact was observed); a comparison between the fits and the experimental data then makes sense in this energy range. In order to enhance the reliability of the fit with $n = 3$, fits with $n = 2$ and $n = 4$ have also been plotted in Fig. 4(a), which definitely shows that we are dealing with a third-order process. Regarding the slow dynamics, the fitting procedure leads to $n = 1$ for $\Delta t = 20$ ps. This result strongly suggests that electrons have been promoted to the conduction band by two independent processes, each of which corresponds to different relaxation dynamics. For both processes, the multiphoton order is lower than the one expected for ideal (D)KDP crystals. Indeed, since the band gap is close to 7.7 eV,[8] five photons would be required for an electron to make a transition from the valence band to the conduction band. From this study, we conclude that a nonnegligible density of SLGs exists in both materials or is rapidly created in the course of interaction. This observation is consistent with first-principles density functional theory calculations, showing that oxygen or hydrogen vacancies induce SLG.[10,11] A schematic illustration of the corresponding band structure and of the two excitation-relaxation processes is given in Fig. 5. Finally, for both KDP and DKDP, we found that the damage threshold for a single-shot laser at 55 fs is 68 TW/cm^2. This result indicates that the fine electronic structure modification due to the isotope influence does not significantly change the photon absorption cross section.

The previous results allow us to make first a hypothesis about the mechanisms involved during and after the laser irradiation. Also, on the basis of previous published scenarios, we tentatively provide interpretations of the experimental data. At 800 nm, the electronic heating is high enough to induce hot electrons ($[H_2PO_4]^- \rightarrow [H_2PO_4]^0 + e^-_{hot}$).[7] This suggests that B radicals (which consist of a STH associated with the [H2PO4]^0 center in KDP - [D2PO4]^0 in DKDP) are involved because, first, a STE may be associated with the STH and,

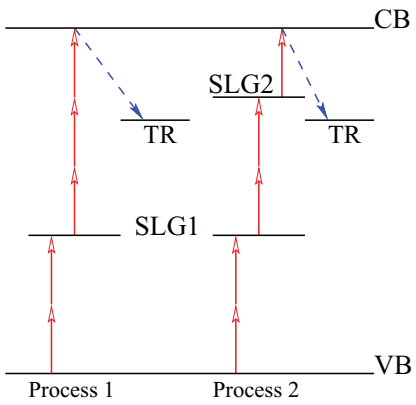

FIG. 5. (Color online) Schematic illustration of the band structure of KDP crystals. Process 1 involving SLG1 corresponds to the fast relaxation dynamics. Process 2 involving the SLG2 corresponds to the slow relaxation dynamics. The solid red arrows indicate the absorption of photons, whereas the dashed blue arrows illustrate the relaxation toward the trapped state TR.

second, the free-hole trapping is intrinsic: the number of recombination centers does not depend on the laser intensity or, subsequently, the trapping rate τ_h^{-1}. [This fact is used in Eq. (3) in Sec. IV.] It follows that many of these electrons can first recombine with holes in a time scale of 300 fs [Eq. (2) in Sec. IV], but a fraction of the excited electrons and holes might relax because of a second mechanism that takes place on a longer time scale. Indeed, the formation time of a hydrogen defect is around 1.6 ps.[17] Thus, the shallow traps can be immediately formed under beam excitation and participate, in turn, to promote the valence electrons to the CB. According to McMillan and Clemens,[7] $[H_2PO_4]^0 + e^- \rightarrow [HPO_4]^- + H$ is effectively a possible second reaction where A radicals are produced. This second process is intensity and isotope dependent and may only need one photon to promote electrons from the states close to the CB. Here the thermalized electrons and holes move independently of each other, and both the electrons and holes can be stabilized in a variety of positive and negative traps.[10,11,16] In particular, the following reactions may take place: $[H_2PO_4]^-$ + free hole $\rightarrow [H_2PO_4]^0$ and, subsequently, $[H_2PO_4]^0$ + free electron $\rightarrow [H_2PO_4]^-$. The latter reaction is governed by the electron-capture cross section σ_c.[7] It is noteworthy that the latter reaction can take place only when the crystalline lattice is relaxed, i.e., when the inverse reaction $[HPO_4]^- + H \rightarrow [H_2PO_4]^-$ has occurred. Also, our measurements show that the relaxation of carriers can last up to 20 ps (KDP) or 40 ps (DKDP), which clearly shows the influence of the isotope, i.e., the relation between the diffusivity coefficient of hydrogen or deuterium and the atom mass, i.e., a migration process. We also suggest an original scenario based on the presence of charged oxygen vacancies that may be implied in the second process since they introduce two SLGs.[11] It is noteworthy that these defects can be present in large concentrations even at room temperature.[4] Also, this defect may significantly enhance the multiphoton absorption cross section and produce a large amount of free electrons (to our knowledge, it has not been shown that STE are associated with oxygen vacancies). Indeed, these $(PO_3)^{2-}$ centers have already been identified as strongly enhancing the absorption.[4] Because of the laser heating, these free electrons can break hydrogen or deuterium bonds, thus producing the A radicals. The following relaxation based on crystalline rearrangements then should be as previously described.

In order to confirm the above-mentioned mechanisms of excitation and relaxation, to interpret finely the experimental data, and to obtain values of the physical quantities involved in these processes, such as the multiphoton ionization or capture cross sections, we have developed a kinetic model with two excitation-relaxation dynamics.

IV. KINETIC MODEL AND DISCUSSION

Let us now develop a kinetic equation system (KES) in order to describe the physical mechanisms responsible for the observed phase shift in the previous section. Also, the aim of the modeling is to describe the response of the sample and to extract quantitative information about the different relaxation processes observed during the experiment.

As an initial remark, we should emphasize the complexity of the behavior observed in both KDP and DKDP crystals, which is much more complex than observed, for instance, in SiO_2 or NaCl. In SiO_2, the fast relaxation of photoexcited carriers is associated with the formation of STEs. The trapping rate (150 fs) is independent of the initial excitation density, and the intensity dependence of the signal just follows the nonlinear evolution expected for a multiphoton transition from the valence band to the conduction band. In NaCl, the situation is slightly more complex but still easy to handle. In this material the formation of STE is also the rule, but this arises through a two-step process: formation of a STH and then trapping of an electron by the STH. This is why we observe an acceleration of the process with an increased excitation density: the higher the density of the STH is, the higher the probability is for an electron to be trapped. In the present case, the overall set of data was much more difficult to interpret because of the important role of SLG. Such a strong influence of empty or occupied defect states has never been observed in other materials by our team, at least at intensities up to the breakdown threshold.

Since all the experimental results show that two relaxation kinetics exist in (D)KDP crystals, we have to introduce two relaxation mechanisms in the rate equations. Since we use moderate intensities that do not produce high carrier densities (no more than 10^{19} cm^{-3}, as will be shown) for which it is reasonable to assume that less than one carrier pair is produced in a cell of the crystalline lattice,[24] we assume that each excitation-relaxation mechanism can be considered as independent of the other. It supposes that free electrons and holes are trapped in the vicinity of the place where they have been produced. Under this assumption, we can derive independent kinetic models for each mechanism. In addition, since the excited carrier density is negligible compared to the density of valence electrons (close to 10^{23} cm^{-3}), the depletion of the valence band is not taken into consideration in the following KES. The comparison of the theoretical predictions with the experimental data will allow, first, stating whether this modeling assumption and the following ones are reliable or not and, second, determining the modeling parameters.

The first relaxation mechanism has no intensity dependence, whereas the characteristic time constant of the second mechanism depends on the intensity. We assume that the first mechanism can be associated with the formation and the trapping of an exciton whose characteristic lifetime τ_1 is a parameter of the model, which can be estimated from the experimental results. It has to be noted that such a description corresponds to the behavior observed in SiO_2. In order to account for the third-order intensity dependence in (D)KDP, we have to assume the presence of a SLG, called SLG1, located roughly at 3.1 eV above the valence band (see Fig. 5). SLG1 is assumed to be initially filled (because it is related to the valence band), and its electronic density does not evolve during the course of interaction, i.e., $n_{\mathrm{SLG1}} = \mathrm{const}$ is imposed. The latter assumption is supported by the fact that SLG1 is filled with an efficient second-order multiphoton process compared to the emptying third-order process, as shown by Fig. 5. The KES corresponding to this first mechanism thus reads

$$\begin{cases} \frac{\partial n_{\mathrm{cb}}^{(1)}}{\partial t} = \sigma_3 F_p^3 n_{\mathrm{SLG1}} - \frac{n_{\mathrm{cb}}^{(1)}}{\tau_1}, \\ \frac{\partial n_{\mathrm{tr}}^{(1)}}{\partial t} = \frac{n_{\mathrm{cb}}^{(1)}}{\tau_1}, \end{cases} \tag{2}$$

where σ_3 is the three-photon absorption cross section to bridge SLG1 to the CB. $n_{\mathrm{cb}}^{(1)}$, n_{SLG1}, and $n_{\mathrm{tr}}^{(1)}$ are the electronic densities in the CB, SLG1, and the trapped state induced by process 1, respectively. F_p is the photon flux given by $I/\hbar\omega$. τ_1 is the relaxation time. Regarding the second mechanism, since both free electrons and holes have been produced, the free holes are first trapped, and subsequently, the free electrons can be trapped by the trapped holes. Also, it is assumed that the free holes are trapped within a characteristic time constant τ_h that accounts for intrinsic hole trapping following laser-induced bond breakings. τ_h then lies in the picosecond time domain. The relaxation time of the free electrons then depends on the trapped-hole population and their ability to be trapped. It turns out that the second mechanism exhibits a behavior close to trends observed in NaCl crystals (see Appendix A). The corresponding KES for (D)KDP thus should mimic the one for NaCl. Such a description would imply that the relaxation time τ_2 can depend on the laser intensity, as shown in Appendix A. More precisely, τ_2 and the maximum of the absolute value of the phase shift $|\Delta\Phi|_{\max}$ are correlated in the sense where both depend on I^n when n photons are required to promote valence electrons to the conduction band (see Appendix A). In (D)KDP crystals, the main difference lies in the fact that the conduction electrons come from the state located in the band gap SLG2 (see Fig. 5) and not directly from the valence band (as shown from the previous analysis of the phase shift evolution with respect to the intensity at $\Delta t = 23$ ps). We thus have to introduce a supplementary rate equation governing the electronic population associated with this additional state SLG2. Since it is just below the conduction band (less than 1.55 eV because the absorption of one photon is enough to induce a transition), it is reasonable to think that this state is related to the conduction band, and thus, we assume it is initially empty, i.e., $n_{\mathrm{SLG2}}(t=0) = 0$. It can be shown that in the case where this state can be filled without any constraint, the density of conduction electrons is not a linear function of the intensity in the general case (see Appendix B). Thus to impose this linear behavior, we have introduced a saturation value n_{sat} that corresponds to the highest electronic density that can be reached during the interaction time, i.e., $n_{\mathrm{SLG2}}(t) < n_{\mathrm{sat}}$ (see Appendix B). The KES for the second mechanism then reads

$$\begin{cases} \frac{\partial n_{\mathrm{cb}}^{(2)}}{\partial t} = \sigma_1 F_p n_{\mathrm{SLG2}} - \sigma_c v n_{\mathrm{cb}}^{(2)}\left(n_{\mathrm{th}}^{(2)} - n_{\mathrm{tr}}^{(2)}\right), \\ \frac{\partial n_{\mathrm{tr}}^{(2)}}{\partial t} = \sigma_c v n_{\mathrm{cb}}^{(2)}\left(n_{\mathrm{th}}^{(2)} - n_{\mathrm{tr}}^{(2)}\right), \\ \frac{\partial n_{\mathrm{fh}}^{(2)}}{\partial t} = \sigma_1 F_p n_{\mathrm{SLG2}} - \frac{n_{\mathrm{fh}}^{(2)}}{\tau_h}, \\ \frac{\partial n_{\mathrm{th}}^{(2)}}{\partial t} = \frac{n_{\mathrm{fh}}^{(2)}}{\tau_h}, \\ \frac{\partial n_{\mathrm{SLG2}}}{\partial t} = \sigma_2 F_p^2 n_{\mathrm{SLG1}} - \sigma_1 F_p n_{\mathrm{SLG2}}, \end{cases} \tag{3}$$

where σ_1 is the one-photon absorption cross section to bridge SLG2 to the CB, σ_2 is the two-photon absorption cross section to bridge SLG1 to SLG2, and σ_c is the electron-capture cross section. v is the average electron velocity (see Ref. 20 for more details), and τ_h is the relaxation time of free holes. $n_{\mathrm{cb}}^{(2)}$, $n_{\mathrm{tr}}^{(2)}$, n_{SLG1}, and n_{SLG2} are the densities of electrons in the CB, in a trapped state, in SLG1, and in SLG2 induced by process 2, respectively. $n_{\mathrm{fh}}^{(2)}$ and $n_{\mathrm{th}}^{(2)}$ are the densities of free and trapped holes induced by process 2, respectively. In the calculation of the phase shift, the free- and trapped-electron populations are given by $n_{\mathrm{cb}} = n_{\mathrm{cb}}^{(1)} + n_{\mathrm{cb}}^{(2)}$ and $n_{\mathrm{tr}} = n_{\mathrm{tr}}^{(1)} + n_{\mathrm{tr}}^{(2)}$, respectively. It is worth noting that the laser-pulse propagation has been taken into consideration in the calculations. Indeed, in its course of propagation, the intensity of the pump pulse can decrease if the carrier absorption is efficient. Since we deal with a long distance ($L = 100\,\mu$m), this effect has to be taken into account. To do so, we use the well-known Beer-Lambert law, where the absorption of both conduction and valence electrons is taken into consideration. The conduction electrons absorption is evaluated with a Drude model, and it has been observed that this is the main contribution to the decrease in the laser intensity as soon as the population of excited carriers is significant.

In order to determine the modeling parameters, we use the fact that the standard phase-shift curves with respect to the time delay exhibit three regions corresponding to different physical mechanisms. First, we have the Kerr effect, which imposes the value of the nonlinear index n_2. The second part of the curves corresponds to the excitation for which no significant relaxation has occurred. This part allows us to set the parameters related to the excitation, for instance, the generalized multiphoton cross sections. Finally, the third part is associated with the relaxation and allows determining the relaxation time or the capture cross section. Also, the modeling parameters corresponding to each of these mechanisms are pretty decorrelated and can be set independently of each other. Following this procedure, we then obtained a set of parameter values that mimic the experimental data. To do so, the model was simultaneously fitted to the six data sets by using a Levenberg-Marquardt algorithm. It is noteworthy that we do not claim the uniqueness of this set. Nevertheless, having only small deviations from the found values allows us to reproduce the experimental data. For the whole intensities, the best fit of the experimental data is obtained with the parameter values summarized in Table I.[25] The obtained phase shifts as a function of the time delay are reported in Fig. 6. Except for the product of the capture cross section with the electron velocity $\sigma_c \times v$, all of these values are the same for both KDP and DKDP crystals. Let us first discuss these values, followed by the comparison between KDP and DKDP.

The obtained generalized multiphoton absorption cross sections are in a fairly good agreement with the empirical formula $\sigma_n = 10^{-19-31(n-1)}\ \mathrm{cm}^{2n}/\mathrm{s}^{n-1}$, where n is the order of the multiphoton transition.[26] The value of τ_1 has been set to 300 fs. This short time confirms we are actually dealing with an exciton: after its promotion, the electron remains linked to its hole, which allows a fast recombination. This phenomenon departs from the one associated with τ_h (describing the second process), whose value has been set to 1 ps. In that case, τ_h accounts for an intrinsic trapping that lies, indeed, as expected in the picosecond time scale (Ref. 20 and references therein). It corresponds to a trapping onto a given radical, and thus, we do not expect a dependence on the isotope. Indeed, we have found that the results of the simulation are not very sensitive to τ_h: several simulations have been realized by taking a few picoseconds instead of 1 ps, but numerical results are always in good agreement with the experimental data. Concerning the electronic density of the SLGs, we have obtained $n_{\mathrm{SLG1}} = n_{\mathrm{sat}} = 2 \times 10^{17}\ \mathrm{cm}^{-3}$. This value is compatible with the density of intrinsic defects that can be

TABLE I. Values of the modeling parameters allowing the best fit of the experimental data for whole intensities.

Parameter	Value	Comment
n_2	1.56×10^{-16} cm^2/W	nonlinear index
σ_1	5×10^{-19} cm^2	one-photon absorption cross section
σ_2	8.1×10^{-50} cm^4/s	two-photon absorption cross section
σ_3	1.3×10^{-82} cm^6/s^2	three-photon absorption cross section
n_{SLG1}	2×10^{17} cm^{-3}	density of defects
n_{sat}	2×10^{17} cm^{-3}	
τ_1	300 fs	associated with the three-photon absorption
$\sigma_c v$ (KDP)	3×10^{-14} cm^2 $\times$ 1.45×10^7 cm/s	value $(\sigma_c v)_{\mathrm{ref}}$ for $I_{\mathrm{ref}} = 42.32$ W/cm^2; with respect to I, we have $\sigma_c v = (\sigma_c v)_{\mathrm{ref}}(I/I_{\mathrm{ref}})^{-3.3}$
$\sigma_c v$ (DKDP)	0.7×10^{-14} cm^2 $\times$ 1.45×10^7 cm/s	value $(\sigma_c v)_{\mathrm{ref}}$ for $I_{\mathrm{ref}} = 36.8$ W/cm^2; with respect to I, we have $\sigma_c v = (\sigma_c v)_{\mathrm{ref}}(I/I_{\mathrm{ref}})^{-3.3}$
τ_h	1 ps	intrinsic hole trapping time
$\hbar\omega_{\mathrm{tr}}$	5.86 eV	trapping energy
f_{cb}	1	free-electron oscillator strength
f_{tr}	1.2	trapped-electron oscillator strength

observed in crystals. Further, according to Liu *et al.*,[11] these defects may correspond to charged oxygen vacancies since they exhibit the same order of magnitude of the electronic density and produce two additional states located in the band gap. Furthermore, the obtained values of n_{SLG1} and n_{sat} are also compatible with the density of defects introduced by Ogorodnikov *et al.*[5] to account for observed decay times. Regarding the trapped state, we have set $\hbar\omega_{\mathrm{tr}} = 5.86$ eV. This value is compatible with luminescence data obtained in the literature.[5] Further, this value renders it possible to likely locate the position of the trapped state in the band structure, as shown in Fig. 5. Finally, the value of the nonlinear index extracted from the experimental data is 1.56×10^{-16} cm^2/W. Because our experimental setup is not designed for measuring this quantity, its value is slightly lower than the standard measured value close to 2.3×10^{-16} cm^2/W.[27]

In order to reproduce well the experimental behavior with respect to the laser intensity, we have also introduced a dependence of $\sigma_c v$ on the intensity as $\sigma_c v \propto I^{-3.3}$. Since $\sigma_c v$ is a function of the conduction electron kinetic energy E_k, this power-law dependence suggests that E_k always depends on I when the trapping event occurs. From a general point of view, $\sigma_c v$ can be proportional to $E_k^{-x} E_k^{1/2}$, where x is a constant. In the case where E_k can be approximated by a power law of the intensity as I^y, then the comparison between experimental data and numerical calculations imposes $(-x + 1/2)y = -3.3$. The reliability of the assumption is supported by the fact that the conduction electrons are strongly heated by the pump laser pulse. Indeed, it can be shown that they can reach a kinetic energy that can be as high as 100 eV (see Appendix C).[28] Further, just after this heating, E_k is proportional to I. When the conduction electrons release their energy (because of electron-phonon collisions), a simple classical description of the evolution of E_k with respect to time allows us to show that E_k remains close to a power law of the intensity as I^y, where $1 < y < 2$ (see Appendix C). Also, the comparison of the modeling results with the experimental data leads to the conclusion that the conduction electron has kept information about its initial energy gain at the trapping moment. Since the trapping occurs in the picosecond time scale, i.e., a long time after the initial laser heating, it can be shown that y may be close to 2 (see Appendix C). From the above-mentioned relation $(-x + 1/2)y = -3.3$, we then deduce that the capture cross section evolves roughly as E_k^{-1}. This exponent is compatible with data available in the literature; see, for instance, Ref. 32.

Let us now come back to the second dynamics associated with the relaxation time τ_2. Calculations give values ranging between 10 and 20 ps. Further, since τ_2 can be approximated by $(\sigma_c v \sigma_1 n_0 I \tau_L)^{-1}$, the intensity dependence of $\sigma_c v$ introduces a departure from the expected typical I^{-1} behavior[20]. In that case it can be shown that $|\Delta\Phi|_{\mathrm{max}}$ and τ_2 are no longer correlated regarding the intensity dependence (different from the study provided in Appendix A).

We finally compare KDP and DKDP results. In order to mimic the experimental difference between them, we have introduced a dependence of σ_c on the isotope.[33] The way we proceed is supported by experimental results given in Ref. 7, where it is shown that the recombination of radicals $[H_2PO_4]^0$ ($[H_2PO_4]^0 + e^- \rightarrow [H_2PO_4]^-$) is faster than the one for [D2PO4]^0 ($[D_2PO_4]^0 + e^- \rightarrow [D_2PO_4]^-$). Actually, this kinetics is governed by a free energy of activation ΔG for recombination of this radical that has been found to be proportional to the relative concentration of deuterium. We interpret this fact as if the recombination time of the free electron depends on the isotope. Actually, we think that the electrons are able to efficiently recombine only when the ionic structure is stabilized, the H-based structure stabilizing faster than the D-based one. This interpretation is consistent with the fact that annealing of $[H_2PO_4]^0$ or $[D_2PO_4]^0$ is related to the freezing of hydrogen or deuterium along the hydrogen or deuterium bond.[7] The capture cross section thus should account for this fact. To take this influence into consideration, we simply change the value of σ_c depending on whether we consider KDP or DKDP crystals. Also, the values of σ_c reported in Table I allow us to reproduce the experimental data. It is worth noting that the larger value of the capture cross

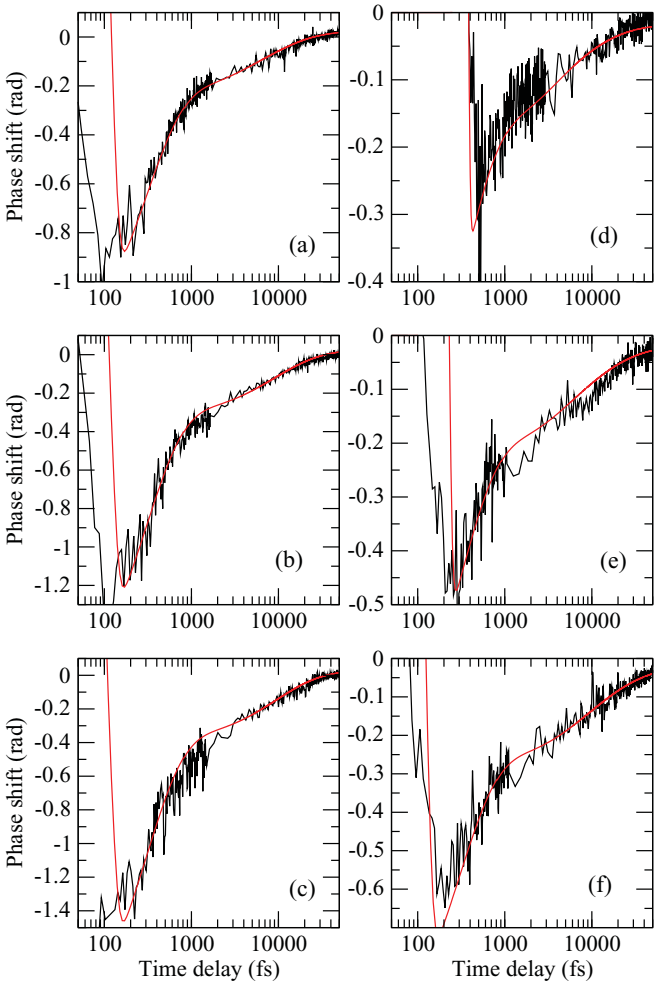

FIG. 6. (Color online) Evolution of the phase shift as a function of the time delay for (left) a KDP crystal and (right) a DKDP crystal for several laser energies: (a) 42.32, (b) 52.47, (c) 59.25, (d) 23.55, (e) 29.07, and (f) 36.8 TW/cm^2. The noisy black curves and the smooth red curves correspond to the experimental data and modeling results based on the resolution of the KES, respectively. Note that a logarithmic scale is used on the horizontal axis in order to underline both relaxation dynamics.

section corresponds to the KDP crystals, and since $\tau_2 \propto \sigma_c^{-1}$, we obtained effectively $\tau_2(\text{KDP}) < \tau_2(\text{DKDP})$.

With the values of the modeling parameters as discussed above, we can reasonably state that a good agreement between experimental data and theoretical predictions is obtained. Further, one can observe that the overall behavior of the phase shift cannot be reduced to a simple combination of exponential functions for describing the decreases. Also, it appears that the KES is able to mimic the complex evolution of the phase shift with respect to time.

Another look at the variations of the phase shift with respect to the laser intensity for a given time delay [Fig. 4(b)] also enhances the reliability of our modeling approach. An extrapolation of the linear fit does not go through the origin, whereas a zero phase shift is expected for a zero intensity. Actually, our modeling allows us to explain the whole evolution of this phase shift with respect to the intensity. For low intensities, SLG2 is not significantly filled in the course of interaction, resulting in a phase shift evolving as I^3 (see Appendix B). For large enough intensities, SLG2 rapidly reaches the saturation density n_{sat}, thus leading to an evolution of the phase shift as I^1 (see Appendix B). Also, as the laser intensity increases, the linear dependence in Fig. 4(b) may come after a cubic one (not measured due to experimental uncertainties), allowing the curve to go through the origin.

On the basis of the models described here, we are able to evaluate the maximum free-electron density produced by the laser pulses. For laser intensities of 23.55 and 52.47 W/cm^2, this density is close to 10^{18} and 10^{19} cm^{-3}, respectively. These orders of magnitude are consistent with previous investigations.[19,20] Furthermore, we confirm *a posteriori* the assumptions made at the beginning of this section.

V. CONCLUSION

In order to study the excitation and the relaxation of carriers in (D)KDP crystals, we have carried out femtosecond time-resolved interferometry. This study has shown that two excitation-relaxation processes exist in KDP and DKDP. Both excitation mechanisms are assisted by the presence of electronic states located in the band gap, leading to a nonlinear dependence upon pump laser intensity that is below the one expected from a direct five-photon transition. The first one results from a third-order process, with a fast relaxation time of 300 fs. This first process has been identified with the formation and relaxation of a self-trapped exciton. The second process corresponds to a signal having a linear dependence upon the laser intensity. The associated relaxation dynamics is much slower than the first process, its time being on a tens of picoseconds time scale. Since this relaxation time depends on the laser intensity and the isotope under consideration, this process is associated with the breaking of hydrogen bonds due to hot free electrons and a subsequent rearrangement of the crystalline lattice. All of these facts have been supported by a model based on a kinetic equation system aimed at describing the time evolution of the electron densities associated with the various states. From this approach, we have been able to obtain more information about the physical mechanisms. Also, we have been able to evaluate the generalized multiphoton absorption cross sections and the capture cross section. The latter has been shown to depend on the electron kinetic energy. In particular, it appeared that the conduction electrons can be heated up to 100 eV.

These results clearly show the existence of states located in the band gap. Also, beyond providing information regarding the fundamental electronic processes in the dielectric material under consideration, the present study confirms the conclusions obtained by two teams in the nanosecond range.[8,15] We further show that the electronic density associated with these states is close to 10^{17} cm^{-3}, which is consistent with previous work.[5] Since oxygen vacancy exhibits states located in the band gap with electronic densities comparable to our values, these defects are believed to be responsible for the observed data. Also, the comparison between the results obtained in both the nanosecond and the femtosecond regime strongly support the fact that oxygen vacancies are involved in laser-induced damage of KDP and DKDP crystals both in the femtosecond and nanosecond regimes. It is noteworthy that in the case of

nanosecond damage where the laser beam is not focused on the sample, the defect responsible for damage may actually be a cluster of holes next to oxygen vacancies induced by the presence of a structural defect.[16,34]

We now plan to perform similar experiments but using the third harmonic of the LUCA facility, corresponding to a wavelength of 266 nm. Since the number of photons required to promote valence electrons to the conduction band is different compared to the present study, different states are expected to be excited. We then expect to obtain more information about the electronic mechanisms that can be excited in KDP or DKDP crystals.

ACKNOWLEDGMENTS

Michèle Raynaud (CEA/IRAMIS/LSI) is gratefully acknowledged for her comments about this manuscript.

APPENDIX A: REVISITED KINETIC MODEL FOR SiO_2 AND NaCl

In Ref. 20, it has been observed for silica that the relaxation time does not depend on the intensity. The KES thus only has to account for a multiphoton excitation and an exponential decay as follows:

$$\begin{cases} \frac{\partial n_{\rm cb}}{\partial t} = \sigma_n F_p^n n_0 - \frac{n_{\rm cb}}{\tau}, \\ \frac{\partial n_{\rm tr}}{\partial t} = \frac{n_{\rm cb}}{\tau}, \end{cases} \tag{A1}$$

where $n_{\rm cb}$ and $n_{\rm tr}$ stand for the conduction and trapped-electron populations, respectively. The term $\sigma_n F_p^n n_0$ describes the production of free particles by the simultaneous absorption of n photons. τ is an effective relaxation time. n_0 is the electronic density in the ground state, which is assumed not to be modified in the course of interaction, i.e., $n_{\rm cb} \ll n_0$.

For NaCl crystals, a dependence of the phase shift with respect to the laser intensity has been observed by Martin *et al.*[20] In order to account for this fact, Martin *et al.* have invoked a two-step relaxation mechanism: since both free electrons and holes have been produced, once the free holes are first trapped, the free electrons can then be trapped by the trapped holes. Also, it is assumed that the free holes are trapped within a characteristic time constant τ_h that accounts for intrinsic hole trapping following laser-induced bond breakings. τ_h also lies in the picosecond time domain. The relaxation time of the free electrons then depends on the trapped-hole population and their ability to be trapped. The kinetic model describing these processes then reads

$$\begin{cases} \frac{\partial n_{\rm cb}}{\partial t} = \sigma_n F_p^n n_0 - \sigma_c v n_{\rm cb}(n_{\rm th} - n_{\rm tr}), \\ \frac{\partial n_{\rm tr}}{\partial t} = \sigma_c v n_{\rm cb}(n_{\rm th} - n_{\rm tr}), \\ \frac{\partial n_{\rm th}}{\partial t} = \frac{n_{\rm fh}}{\tau_h}, \\ \frac{\partial n_{\rm fh}}{\partial t} = \sigma_n F_p^n n_0 - \frac{n_{\rm fh}}{\tau_h}, \end{cases} \tag{A2}$$

where $n_{\rm cb}$, $n_{\rm tr}$, $n_{\rm fh}$, and $n_{\rm th}$ stand for the densities of free electrons in the conduction band, trapped electrons, free holes, and trapped holes, respectively. The electron trapping efficiency is described by the product $\sigma_c v$, where σ_c is the electron-capture cross section and v is its velocity. τ_h^{-1} is an intrinsic hole trapping rate. Let us now evaluate the behavior of the physical parameters of interest for us with respect to the laser intensity. Regarding the maximum of the absolute phase shift amplitude, since it corresponds to a situation for which no significant relaxation has occurred, it is mainly related to the free-electron density, which is proportional to the production term. It follows that

$$|\Delta\Phi|_{\rm max} \propto I^n. \tag{A3}$$

Concerning the electron relaxation time $\tau_{\rm eff}$, its instantaneous expression is given by the inverse of $\sigma_c v(n_{\rm th} - n_{\rm tr})$. Also, the larger the number of available trapped holes is, the faster the relaxation is. In the case where not too many electrons have been trapped, $(n_{\rm th} - n_{\rm tr})$ can be approximated by $n_{\rm th}$, the latter population being proportional to I^n. [This can be shown by solving exactly the hole rate equations of Eq. (A2).] It follows that

$$\tau_{\rm eff} \propto \frac{1}{\sigma_c v \sigma_n F_p^n n_0} \propto \frac{1}{I^n}. \tag{A4}$$

From the previous considerations, it appears clearly that $|\Delta\Phi|_{\rm max}$ and $\tau_{\rm eff}$ are correlated because both of them depend on the same power of the laser intensity.

APPENDIX B: ROLE OF AN INTERMEDIATE STATE ON THE INTENSITY DEPENDENCE OF THE FREE-ELECTRON POPULATION

Let us consider the promotion of valence electrons into the conduction band assisted by an intermediate state (see Fig. 7). We assume the promotion to be a two-step process where the transition from the valence band to the intermediate state and the transition from the intermediate state to the conduction band result from the absorption of n and m photons, respectively. The electrons are assumed to pass through the intermediate state during a certain time. The resulting rate equations during the course of interaction are

$$\begin{cases} \frac{\partial n_{\rm cb}}{\partial t} = \sigma_m F_p^m n_{\rm SLG} - \frac{n_{\rm cb}}{\tau} \\ \frac{\partial n_{\rm SLG}}{\partial t} = \sigma_n F_p^n n_{\rm vb} - \sigma_m F_p^m n_{\rm SLG}, \end{cases} \tag{B1}$$

where τ is an effective relaxation time. It is assumed that the variations of $n_{\rm vb}$ are negligible, i.e., $n_{\rm SLG}(t) \ll n_{\rm vb}$ and $n_{\rm cb}(t) \ll n_{\rm vb}$ for all times. This system can be solved exactly,

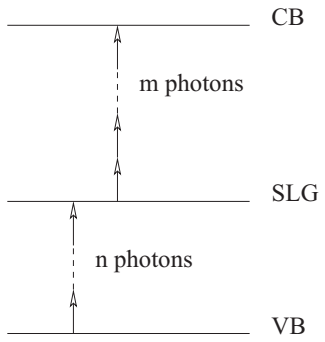

FIG. 7. Schematic band structure including one state located in the gap. VB and CB denotes the valence band and the conduction band, respectively. n photons are required to bridge the VB to the SLG, whereas m photons are required to bridge the SLG to the CB.

and with $n_{\mathrm{SLG}}(t=0) = n_{\mathrm{cb}}(t=0) = 0$ as initial conditions, we obtain

$$n_{\mathrm{SLG}}(t) = \frac{\sigma_n F_p^n n_{\mathrm{vb}}}{\sigma_m F_p^m}\left(1 - e^{-\sigma_m F_p^m t}\right) \tag{B2}$$

and

$$n_{\mathrm{cb}}(t) = \sigma_n F_p^n n_{\mathrm{vb}}\left[\tau(1 - e^{-t/\tau}) - \frac{e^{-\sigma_m F_p^m t} - e^{-t/\tau}}{\tau^{-1} - \sigma_m F_p^m}\right]. \tag{B3}$$

If the electronic population associated with the intermediate state does not reach any saturation, i.e., $\sigma_m F_p^m t \ll 1$, then expression (B3) transforms into

$$n_{\mathrm{cb}}(t) \simeq \sigma_m \sigma_n F_p^{m+n} n_{\mathrm{vb}}\left[\frac{\tau t - \tau^2(1 - e^{-t/\tau})}{1 - \sigma_m F_p^m \tau}\right]. \tag{B4}$$

In this case, we thus have roughly $n_{\mathrm{cb}} \propto I^{m+n}$. In the case where n_{SLG} rapidly reaches a certain value n_{sat} in the course of interaction, such that n_{SLG} cannot exceed n_{sat}, the resolution of the differential equation governing $n_{\mathrm{cb}}(t)$ in Eq. (B1), where n_{SLG} is replaced by the constant n_{sat}, leads to

$$n_{\mathrm{cb}}(t) \simeq \sigma_m F_p^m n_{\mathrm{sat}} \tau(1 - e^{-t/\tau}) \tag{B5}$$

and, subsequently, $n_{\mathrm{cb}} \propto I^m$. Also, the introduction of a saturation density allows us to lose any information on how the intermediate state has been filled. This fact allows us to explain simply why n_{cb} exhibits a low-order dependence on the intensity when SLGs are present.

APPENDIX C: CONSIDERATIONS ABOUT THE KINETIC ENERGY OF THE CONDUCTION ELECTRONS

Here we address the evolution of the kinetic energy E_k of the conduction electron as a function of time. In particular, we analyze its behavior with respect to the laser intensity I. When the conduction electrons are accelerated in the electric field of the laser pulse, they are heated up to an energy E_{k0} that can be evaluated with a Drude model. This energy reads

$$E_{k0} = \frac{e^2}{c\varepsilon_0 m^*}\frac{\nu_c \tau_L}{\omega^2 + \nu_c^2} I, \tag{C1}$$

where ν_c is the collisional frequency between electrons and phonons, τ_L is the pulse duration, and e, ε_0, m^*, and c denote the usual fundamental constants. An estimation of E_{k0} is obtained by taking $\nu_c = 10^{15}$ s^{-1} and $I = 10$ TW/cm^2. We find $E_{k0} \simeq 100$ eV. Since the laser pulse has switched off, the conduction electrons release their energy into the lattice through collisions with phonons. Let us now analyze the electron energy decrease with respect to time. Since we are dealing with electrons carrying a relatively large energy, we adopt a classical description that allows us to provide trends. For every collision, the electron loses the energy of a phonon U_{ph}. We assume that this event occurs with a frequency $\nu_{e-\mathrm{ph}}$. We obtain

$$E_k(t) = E_{k0} - \nu_{e-\mathrm{ph}} U_{\mathrm{ph}} t = E_{k0} - \alpha E_k^{1/2}(t) U_{\mathrm{ph}} t, \tag{C2}$$

where α is a constant. It has been assumed that $\nu_{e-\mathrm{ph}}$ is proportional to the electron velocity v, and the relation $E_k = mv^2/2$ has been used. Simple algebra allow us to determine an explicit expression of $E_k(t)$ from Eq. (C2).We obtain

$$E_k(t) = \frac{1}{4}\left(\sqrt{(\alpha U_{\mathrm{ph}} t)^2 + 4E_{k0}} - \alpha U_{\mathrm{ph}} t\right)^2. \tag{C3}$$

$E_k(t)$ indeed decreases monotonically as a function of time. For the shortest times, of course, we find $E_k(t = \tau_L) \simeq E_{k0}$ and thus $E_k(t = \tau_L) \propto I$. For times for which $E_k(t)$ goes to zero, i.e., $t \gg 2\sqrt{E_{k0}/\alpha U_{\mathrm{ph}}}$, we can show that $E_k(t) \to (E_{k0}/\alpha U_{\mathrm{ph}} t)^2$ and thus $E_k(t) \propto I^2$ in this case. From these two boundary cases, we can thus approximate the behavior of $E_k(t)$ with respect to the intensity to be I^y, with y in the interval $[1; 2]$. It is noteworthy that the previous considerations about the intensity dependence of $E_k(t)$ remain valid as long as $E_k(t) > U_{\mathrm{ph}}$. If not, quantum effects become dominant. Moreover, in the case where $E_k(t)$ goes down to U_{ph}, $E_k(t)$ no longer depends on the intensity.

*guillaume.duchateau@cea.fr

[1] J. D. Yoreo, A. Burnham, and P. Whitman, Int. Metall. Rev. **47**, 113 (2002).

[2] M. Chirila, N. Garces, L. Halliburton, S. Demos, T. Land, and H. Radousky, J. Appl. Phys. **94**, 6456 (2003).

[3] S. D. Setzler, K. T. Stevens, L. E. Halliburton, M. Yan, N. P. Zaitseva, and J. J. DeYoreo, Phys. Rev. B **57**, 2643 (1998).

[4] N. Y. Garces, K. T. Stevens, L. E. Halliburton, S. G. Demos, H. B. Radousky, and N. P. Zaitseva, J. Appl. Phys. **89**, 47 (2001).

[5] I. Ogorodnikov, V. Yakovlev, B. Shul'gin, and M. Satybaldieva, Phys. Solid State **44**, 880 (2002).

[6] K. Stevens, N. Garces, L. Halliburton, M. Yan, N. Zaitseva, J. DeYoreo, G. Catella, and J. Luken, Appl. Phys. Lett. **75**, 1503 (1999).

[7] J. McMillan and J. Clemens, J. Chem. Phys. **68**, 3627 (1978).

[8] C. W. Carr, H. B. Radousky, and S. G. Demos, Phys. Rev. Lett. **91**, 127402 (2003).

[9] C. W. Carr, H. B. Radousky, A. M. Rubenchik, M. D. Feit, and S. G. Demos, Phys. Rev. Lett. **92**, 087401 (2004).

[10] C. S. Liu, N. Kioussis, S. G. Demos, and H. B. Radousky, Phys. Rev. Lett. **91**, 015505 (2003).

[11] C. S. Liu, C. J. Hou, N. Kioussis, S. G. Demos, and H. B. Radousky, Phys. Rev. B **72**, 134110 (2005).

[12] M. D. Feit, A. M. Rubenchik, and J. B. Trenholme, Proc. SPIE **5991**, 59910W (2005).

[13] G. Duchateau and A. Dyan, Opt. Express **15**, 4557 (2007).

[14] A. Dyan, F. Enguehard, S. Lallich, H. Piombini, and G. Duchateau, J. Opt. Soc. Am. B **25**, 1087 (2008).

[15] S. Reyné, G. Duchateau, J.-Y. Natoli, and L. Lamaignère, Appl. Phys. Lett. **96**, 121102 (2010).

[16] S. Demos, R. Negres, P. Demange, and M. Feit, Opt. Express **18**, 13788 (2010).

[17] J. Davis, R. Hughes, and H. Lee, Chem. Phys. Lett. **207**, 540 (1993).

[18]C. Carr, M. Feit, A. Rubenchik, P. DeMange, S. Kucheyev, M. Shirk, H. Radousky, and S. Demos, Opt. Lett. **30**, 661 (2005).
[19]S. Guizard, P. Martin, P. Daguzan, G. Petite, P. Audebert, J. Geindre, A. D. Santos, and A. Antonetti, Europhys. Lett. **29** 401 (1995).
[20]P. Martin, S. Guizard, P. Daguzan, G. Petite, P. D'Oliveira, P. Meynadier, and M. Perdrix, Phys. Rev. B **55**, 5799 (1997).
[21][http://iramis.cea.fr/slic].
[22]C. D. Marshall, S. A. Payne, M. A. Henesian, J. A. Speth, and H. T. Powell, J. Opt. Soc. Am. B **11**, 774 (1994).
[23]M. S. Pshenichnikov, A. Baltuska, and D. A. Wiersma, Chem. Phys. Lett. **389**, 171 (2004).
[24]An electronic density of 10^{19} cm^{-3} corresponds to an average length between electrons close to 5 nm. Since the lattice cell size is smaller than 1 nm in KDP crystals, a STE localized in a cell then is assumed not to interact with other defects.
[25]It is noteworthy that results based on the previous KES can be slightly improved by also considering an additional KES. Its structure is the same as Eq. (2). It accounts for a direct transition from the valence band to the conduction band with the absorption of five photons and a constant relaxation time close to 9 ps.
[26]P. Agostini and G. Petite, Contemp. Phys. **29**, 57 (1988).
[27]R. A. Ganeev, I. A. Kulagin, A. I. Ryaasnyansky, R. I. Tugushev, and T. Usmanov, Opt. Commun. **229**, 403 (2004).
[28]Although the electrons can reach kinetic energies up to 100 eV, collisional ionization is not expected to play a significant role in the ionization. Indeed, avalanche requires a certain time to engage. Within our laser parameters, this time is too long.[29–31] Furthermore, when electronic avalanche due to impact ionization is significant compared to multiphoton ionization, the free-electron density evolves exponentially with respect to the laser intensity. Since this behavior is not experimentally observed ($\Delta\Phi$ evolves as a given power of the intensity), this shows impact ionization does not play a significant role in the ionization. Therefore, this ionization mechanism has not been included in the modeling.
[29]V. V. Temnov, K. Sokolowski-Tinten, P. Zhou, A. El-Khamhawy, and D. von der Linde, Phys. Rev. Lett. **97**, 237403 (2006).
[30]F. Quéré, S. Guizard, and P. Martin, Eur. Phys. Lett. **56**, 138 (2001).
[31]B. Rethfeld, Phys. Rev. B **73**, 035101 (2006).
[32]R. Heppner, F. Walls, W. Armstrong, and G. Dunn, Phys. Rev. A **13**, 1000 (1976).
[33]The kinetic equations only account for the population of the carriers. So they cannot describe explicitly the ion's mobility. This goal then is achieved by introducing an implicit dependence on the isotope in σ_c.
[34]G. Duchateau, Opt. Express **17**, 10434 (2009).